

Soft Matter

Accepted Manuscript



This is an *Accepted Manuscript*, which has been through the Royal Society of Chemistry peer review process and has been accepted for publication.

Accepted Manuscripts are published online shortly after acceptance, before technical editing, formatting and proof reading. Using this free service, authors can make their results available to the community, in citable form, before we publish the edited article. We will replace this *Accepted Manuscript* with the edited and formatted *Advance Article* as soon as it is available.

You can find more information about *Accepted Manuscripts* in the [Information for Authors](#).

Please note that technical editing may introduce minor changes to the text and/or graphics, which may alter content. The journal's standard [Terms & Conditions](#) and the [Ethical guidelines](#) still apply. In no event shall the Royal Society of Chemistry be held responsible for any errors or omissions in this *Accepted Manuscript* or any consequences arising from the use of any information it contains.

ARTICLE

Capillarity-induced directed self-assembly of patchy hexagram particles at the air-water interface

Cite this: DOI: 10.1039/x0xx00000x

Sung-Min Kang^a, Chang-Hyung Choi^a, Jongmin Kim^a, Su-Jin Yeom^a, Daeyeon Lee^c, Bum Jun Park^b, and Chang-Soo Lee^{a,*}

Received 00th March 2016,
Accepted 00th March 2016

DOI: 10.1039/x0xx00000x

www.rsc.org/

Directed self-assembly can produce ordered or organized superstructures from pre-existing building blocks through pre-programmed interactions. Encoding desired information into building blocks with specific directionality and strength, however, poses a significant challenge for the development of self-assembled superstructures. Here, we demonstrate that controlling the shape and patchiness of particles trapped at the air-water interface can represent a powerful approach for forming ordered macroscopic complex structures through capillary interactions. We designed hexagram particles using a micromolding method that allowed for precise control over the shape and, more importantly, the chemical patchiness of the particles. The assembly behaviors of these hexagram particles at the air-water interface were strongly affected by chemical patchiness. In particular, two-dimensional millimeter-scale ordered structures could be formed by varying the patchiness of the hexagram particles, and we attribute this effect to the delicate balance between the attractive and repulsive interactions among the patchy hexagram particles. Our results provide important clues for encoding information into patchy particles to achieve macroscopic assemblies via a simple molding technique and potentially pave a new pathway for the programmable assembly of particles at the air-water interface.

Introduction

Self-assembly is a process that lowers the Gibbs free energy of a system, leading to the spontaneous organization of matter to attain an equilibrium state.¹⁻⁴ Self-assembly is a promising route for the fabrication of novel functional materials and architectures across multiple length scales. There has been substantial progress in the development of approaches to self-assemble micro and nanoscale materials into macroscopic suprastructures.⁵⁻⁷ The self-assembly of colloidal particles, for example, has led to the formation of suprastructures that exhibit unique organization and functionality.⁸⁻¹¹ Examples include photonic materials generated via the self-assembly of micron-sized colloidal particles and binary nanoparticle superlattices (BNSL) assembled with nanoparticles of different chemical compositions and geometries.¹²⁻¹⁵ Patchy spherical colloids have also been used as elementary building blocks to induce the formation of two-dimensional Kagome lattices.¹⁶ Particle assemblies serve as excellent model systems to analyze and understand the organization and behavior (e.g., crystals, glasses, coordination compounds, proteins, and nucleic acids) of atomic and molecular systems.¹⁷⁻²¹

Despite significant developments in this area of research, many conceptual and technical limitations in controlling the directionality and/or programmability of assemblies persist.²² In particular, instructions and guidance enabling the reproducible formation of designed suprastructures from basic building blocks remain lacking. The information about a desired assembly must specify the directionality of the interactions and

the strength of the building blocks. In fact, one of the key features enabling atomic and molecular assemblies is the ubiquity of anisotropic and directional bonding between atoms and molecules allowing for the formation of complex structures with useful functionalities.²³⁻²⁸ Directional bonding among “simple” carbon atoms, for example, leads to well-ordered structures, such as diamond and graphite.²⁹⁻³¹ The two-dimensional confinement of carbon atoms, in particular, leads to the formation of graphene, which has remarkable properties that are being exploited for advanced applications in electronics, composite materials and separation processes.³²⁻³⁵ The directional interaction of carbon atoms and their organization into two-dimensional crystalline structures, such as graphene, in particular, serves as a basis for devising approaches to harness the directional bonding of colloidal systems to attain analogous two-dimensional assemblies.

Interfaces between two immiscible fluids, such as air and water or oil and water, represent ubiquitous platforms to induce the two-dimensional directed assembly of particles of various shapes and functionalities.³⁶⁻⁴¹ In particular, the assembly of particles driven by interface deformation and the resulting capillarity demonstrates the enormous potential for achieving unique two-dimensional particle assemblies.⁴²⁻⁴⁶ The interface deformation around particles confined at a fluid-fluid interface induces capillary interactions between the particles, reducing the excess surface area and, thus, the total free energy of the system. For example, it has been demonstrated that the curvature of an interface can direct the assembly of particles to specific locations over large length scales (i.e., typically a few

orders of magnitude larger than the size of the particles).⁴⁷⁻⁵² Despite recent progress in this area, few reports have provided convincing evidence of the use of capillarity to direct the assembly of interface-trapped particles into macroscopic two-dimensional regular arrays. This difficulty partly lies in the fact that only particles with relatively simple shapes and chemical heterogeneity have been explored for directed assembly to date.

In this work, we demonstrate the directed self-assembly of patchy hexagram particles into a macroscopic array at an air-water interface. Specifically, this study reveals that solely controlling the shape of the particles may not be sufficient to induce desired assemblies; instead, the precise control of both the shape and patchiness of the particles is necessary to achieve the large-scale assembly of particles at the fluid interface. We investigate the effects of geometric and chemical patchiness on the assembly behavior of hexagram particles at the interface. Shape and chemical anisotropy induce deformation of the air-water interface, which results in orientation-dependent attractions and repulsions leading to the formation of macroscopic particle assemblies with preferred orientations. Our results provide important design criteria for directing and programming the assembly of particles at fluid interfaces to create suprastructures with desired properties and functionalities.

Experimental section

Preparation of hexagram particles

A basic protocol for the micromolding technique was used to synthesize anisotropic patchy hexagram particles from photocurable solutions with tunable patch sizes, following the particle replication in nonwetting templates (PRINT) method.⁵³ The detailed experimental procedure is described in Fig. S1, S2 and S3. Briefly, a relatively weak hydrophobic prepolymer solution (trimethylolpropane triacrylate (TMPTA) in ethanol) for the patch region was loaded on a hexagram polydimethylsiloxane (PDMS) micromold fabricated by soft lithography.⁵⁴ After removal of the excess prepolymer solution from the micromold, ethanol was allowed to evaporate at 80 °C in an oven for 3 min. Partial photopolymerization was performed via 365 nm UV exposure for 30 sec in a nitrogen chamber. After filling the remaining micromold cavities with a second prepolymer solution (poly(ethylene glycol)-diacrylate (PEG-DA)), thereby partitioning the stronger hydrophilic body region of the hexagram particle, complete polymerization was achieved by intense UV irradiation for 90 sec (approximately 20 J/cm² power) in a nitrogen chamber. Also, the homogeneous hexagram particle is fabricated in the same way without prepolymer dilution step. A hydrophilic and/or hydrophobic prepolymer solution was loaded on a hexagram micromold. After removal of the excess prepolymer solution, complete polymerization was performed by UV irradiation for 90 sec in nitrogen chamber. All of the resulting hexagram particles were sequentially harvested, washed, and dispersed in ethanol.

Measurements of pair interactions

The attractive interactions between two hexagram patchy particles at the air-water interface were measured by analyzing their trajectories. A small number of particles dispersed in water were spread on an air-water interface. The sequential images were recorded using a high-speed camera (Phantom Miro eX2, Vision Research, USA) at a frame rate of 300

frames/s as two adjacent particles approached each other and made contact at $t = t_{max}$. The particle trajectories, the corresponding center-to-center separation (r) values, and relative velocities were then calculated using ImageJ software and the particle-tracking method.⁵⁵ Because the particle behaviors were in the low Reynolds number limit ($N_{Re} = (2Rv\rho)/\mu \ll 1$, where ρ and μ are the density and viscosity of the fluid, respectively), a linear relationship between the interaction force ($F \sim r^{\beta-1}$) and the drift velocity ($v = dr/dt$) could be assumed. From the two relationships of $\log r \sim \alpha \log t$ and $\log t \sim (2 - \beta) \log r$, the power law exponent (β) of the interaction force could be related to the value of α , resulting in $\beta = 2 - 1/\alpha$.⁵⁶

Analysis of interface deformation around particles

Optical profilometry (NanoFocus AG, Germany) was used to observe the configurations of the patchy hexagram particles and the profile of interface deformation around the patchy hexagram particles at the air-water interface. The profilometry was based on white light interferometry in which an interferometric objective was mounted on a scanning device that moved vertically. A 3D interferogram was rendered by the detection of interferogram intensities.

Results and discussion

Directed assembly of patchy hexagram particles

Each patchy hexagram particle, which was prepared by a micromolding technique,⁵⁷⁻⁵⁹ was made of a hydrophilic main body (polyethylene glycol-diacrylate (PEG-DA)) and six hydrophobic patches (trimethylolpropane triacrylate (TMPTA)) located at the vertices of the hexagram (see Experimental section and Supplementary information). Homogeneously hydrophilic or hydrophobic hexagram particles with uniform surface chemistries were also investigated. The hexagram shape was inspired by recent results that have demonstrated the spontaneous formation of one-dimensional chains from chemically homogeneous cylinders at fluid interfaces.³⁶⁻³⁸

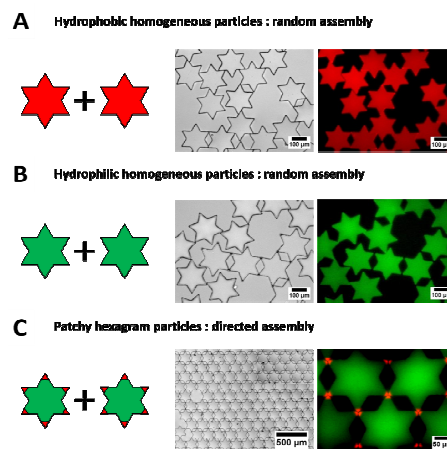


Fig. 1 Directed assembly of patchy hexagram particles at the air-water interface. (A) Hydrophobic homogeneous particles, (B) hydrophilic homogeneous particles, and (C) patchy hexagram particles containing hydrophobic vertices and hydrophilic main hexagram bodies.

The interface deformation around these anisotropic particles was shown to lead to deterministic one-dimensional assembly. Thus, it seemed highly plausible that chemically homogenous hexagrams would self-assemble into a two-dimensional hexagonal lattice induced by interface deformation around the sharp tip of each vertex (i.e., hexagonal interface deformation around each particle). Interestingly, although smaller clusters of regular assemblies were observed, overall, the chemically uniform hexagram particles aggregated to form random arrays of particles, regardless of their surface wettability (Fig. 1A and B). Particle assembly at the interface was likely driven to minimize the interfacial free energy of the system, which could have been partially achieved by clustering the particles and reducing the interfacial area in the system. We note that the Bond number of these patchy hexagram particles is approximately $\sim 10^{-2}$, which indicates that gravity-induced interface deformation is negligible.^{38,51,60} In stark contrast, we observed strong indications of directional interactions that led to the formation of a two-dimensional ordered superstructure when a particular set of patchy hexagram particles were spread across the air-water interface (Fig. 1C). We found that amphiphilic hexagram particles with hydrophilic main bodies and small hydrophobic patches at the tips of the hexagram vertices assembled into a macroscopic hexagonal lattice suprastructure. These results suggest the importance of controlling both the shape and chemical heterogeneity of particles to induce their ordered assembly at the fluid-fluid interface.

Effect of patch size on the assembly structure

To better understand the effect of chemical heterogeneity on the assembly behavior of interface-trapped hexagrams, we investigated the effect of patch size on the assembly of hexagrams at the air-water interface. We prepared hexagram particles with varying hydrophobic patch sizes using the micromolding method (Fig. 2B and Fig. S2 and S3).

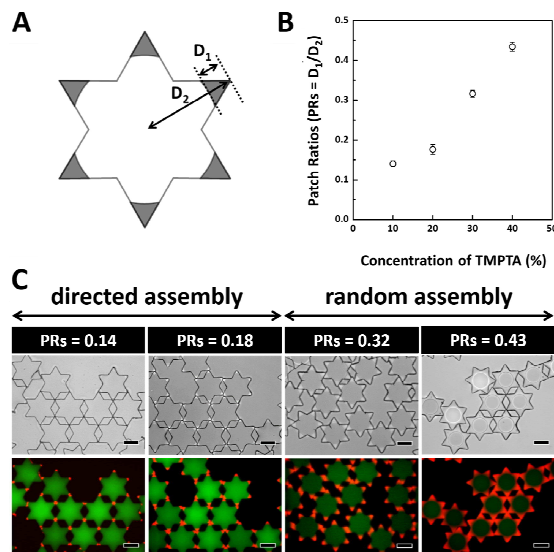


Fig. 2 Effect of patch size on the assembly structure of particles at the air-water interface. (A) A typical feature of patchy hexagram particles is the ratio of hydrophobic patches and hydrophilic bodies, termed the patch ratios ($PRs = D_1/D_2$). (B) The control of $PRs (D_1/D_2)$ in the patchy hexagram particles. (C) The assembly behavior of patchy hexagram particles and its dependence on the $PRs (D_1/D_2)$ at the air-water interface. The scale bars are 100 μm .

Inspired by the hydrophile-lipophile balance (HLB) that is widely used to quantify the amphiphilicity of molecular surfactants, we defined the balance between the hydrophobic and hydrophilic regions of patch hexagram particles using “patch ratios (PRs),” expressed as D_1/D_2 (Fig. 2A).⁶¹ As shown in Fig. 2C, hexagram particles with relatively small patches ($D_1/D_2 = 0.14$ and 0.18) organized into two-dimensional ordered arrays, in which the vertices of the hexagrams contacted those of other particles (Fig. 2C and Fig. S4). In contrast, the assembly of particles with larger patches ($D_1/D_2 = 0.32$ and 0.43 made with 30% and 40% of TMPTA solutions, respectively) was found to be less organized and produced disordered or random assembly structures (Fig. 2C). These results illustrate that there is an optimal range of patch sizes that leads to the ordered assembly of hexagram particles at the air-water interface. Neither hexagrams with homogeneous surface chemistry nor those with large patches organized into long-range ordered structures.

Assembly configuration of patchy hexagram particles

To further probe the effects of patch ratios ($PRs = D_1/D_2$) on the assembly behavior of particles, we monitored the assembly of hexagram particle pairs at the air-water interface. Specifically, we analyzed the “bonding” configuration between two hexagrams using the following three categories: tip-to-tip, tip-to-side, and side-to-side. Notably, all of these bonds were made between hydrophobic patches of interacting hexagrams. When hexagrams with small patches ($PRs = 0.14$ and 0.18) were attracted to each other, the tips of vertices made contacts in most pairs; that is, most hexagrams form tip-to-tip bonds (Fig. 3A-C). While there may have been rotational rearrangements of particles to bring neighboring tips together to form additional tip-to-tip bonds, the tips that were in contact with other tips did not lose their tip-to-tip bonds, even after 24 hours. Even the hexagram pairs that did not form tip-to-side bonds had their tips very close to each other. In contrast, when a pair of hexagrams with large patches ($PRs = 0.32$ and 0.43) approached each other, a large fraction of the particles primarily coordinated with other particles in the tip-to-side configuration. Some of these particles rotated and/or slid with each other to form side-to-side configurations (Fig. 3D-F). Most of the particles that originally formed tip-to-tip bonds underwent translational and rotational rearrangements to form side-to-side bonds, as shown by the data collected 24 hours after initial contact. Based on these results, we hypothesized that the effect of patch size on the assembly behavior of particles was closely related to the sharpness of local interface deformation around the vertices. Interface deformation caused by an interface-trapped particle is known to strongly depend on the geometry and surface wettability of the particle. For the patchy particles with $PRs = 0.14$ and 0.18 , interface deformation was mainly focused on the vertices. The capillarity caused by such sharp interface deformation directed the particles to make contact predominantly in the tip-to-tip configuration, which significantly decreased the interfacial area and, thus, the surface free energy of the system (Fig. 3A and B); this led to the formation of a well-ordered assembly structure, as shown in Fig. 2C. In contrast, for the hexagrams with large patches, the absence of sharpness of the interface deformation around the vertices resulted in diverse and heterogeneous bond formation between the hexagrams. Similar random structures were also observed for the hexagram particles without patches at the air-water interface (Fig. 2C), suggesting that the interface deformation around these

chemically homogeneous particles may not have been sharp enough to induce the ordered assembly of particles (Fig. 1A and B).

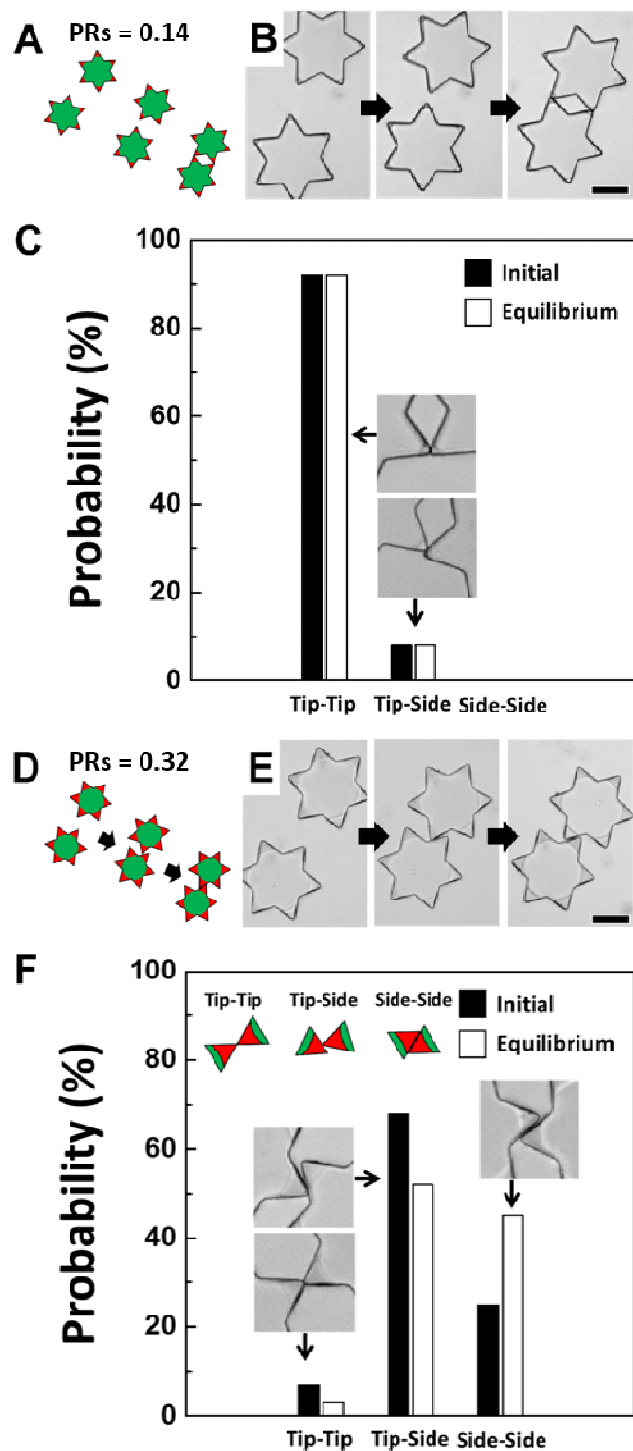


Fig. 3 Assembly configuration of patchy hexagram particles. (A) Schematic illustration and (B) bright-field micrograph of tip-to-tip interactions for PRs = 0.14. (C) Probabilities of pair interactions with PRs = 0.14. (D) Schematic illustration and (E) bright-field micrograph of side-to-side interactions for PRs = 0.32. (F) Probabilities of pair interactions with PRs = 0.32. The scale bars indicate 100 μm .

Sharpness effect of interface deformation on assembly behaviors

To corroborate our hypotheses, we analyzed the interface profiles around hexagram patchy particles at the air-water interface using a gel-trapping method.⁶² Hexagram particles were spread at the air-water interface at 50 $^{\circ}\text{C}$ where the aqueous phase contained 2 wt % gellan. After cooling the sample under ambient conditions, gelation of the aqueous phase occurred such that the particles were immobilized on the gel surface. An optical profilometer was used to scan the height profile of the gelled sample. The profilometry results supported our hypotheses. The interface menisci around the patches, regardless of PRs (D_1/D_2), were found to be deflected downward around the vertex regions (negative deformation), whereas the interface formed raised menisci in the cleavage region between the patches (positive deformation) (Fig. 4).

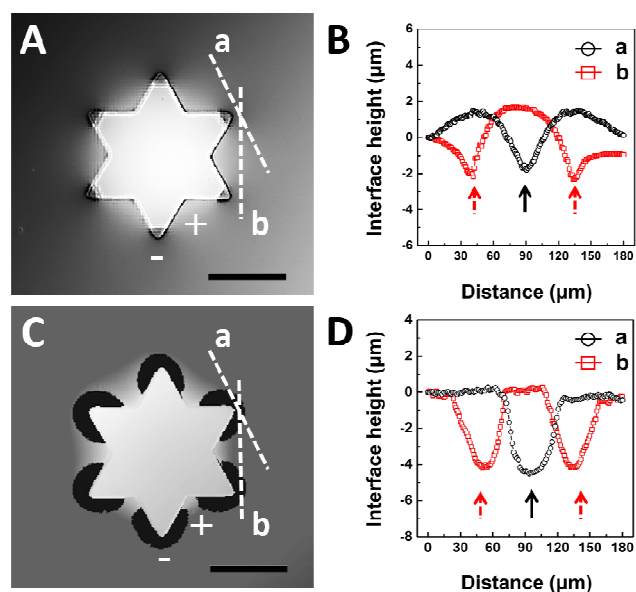


Fig. 4 Interface deformation profiles around the patchy hexagram particles at the air-water interface. Optical profilometry images of PRs = (A) 0.14 and (C) 0.32. The scale bars indicate 100 μm . (B) and (D) The heights of the interface deformation were obtained from the dashed lines (a) and (b), respectively.

However, the negative deformation around a large patch was rather diffuse compared to that around a small patch (dark regions in Fig. 4). As hypothesized, the small patch at the tip of a vertex seemed to be a critical feature that focused and magnified the deformation of the negative interface and, in turn, enabled the assembly of the ordered array of patchy hexagrams. In addition, our results suggested that the shape of the particles themselves may not have been enough to direct the particles into two-dimensional ordered suprastructures, as evidenced by the failure of chemically homogeneous hexagrams to form regular arrays (Fig. S5). The random assembly behaviors of homogeneous particles have been attributed from an undulated contact line at the particle surface of each homogeneous particle, which can be described as capillary interaction between capillary multipoles in the presence of surface roughness (Fig. S6 and S7). The contact-line undulations produce distortions in the surrounding liquid interface, whose overlap engenders capillary interaction between the particles.^{51,56,63,64}

Pair interactions between patchy hexagram particles

The fact that hexagrams with small patches were able to arrange into long-range ordered suprastructures indicated that their interactions were highly directional. One way to probe such directionality was to probe the mode of the capillary attractions by determining the pair interactions (U) (Fig. 5A). The trajectories of hexagrams with small patches (i.e., the particles that arranged into ordered suprastructures) obtained from high-speed imaging were used to infer their pair potentials (U) using a previously reported approach.⁶⁵

As shown in Fig. 5B, the center-to-center separation (r) as a function of time ($t_{max} - t$) consistently decayed with a power law exponent of $\alpha \approx 0.07$ in the far-field linear regimes of the log-log plot where $r = (t_{max} - t)^\alpha$. The value of α is related to the scaling behavior of the capillary attraction via $U \sim r^\beta$ in which $\beta = 2 - 1/\alpha \approx -12.3$.^{43, 44, 47-51} According to the results, we believe that the interaction range between the patchy hexagram particles does not depend on the patchy size of hexagram particles.

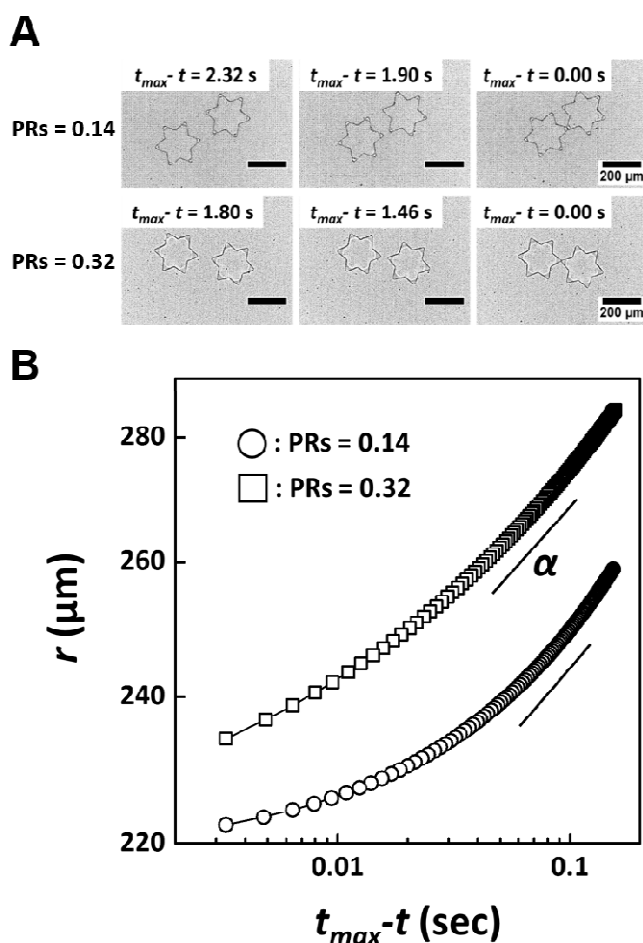


Fig. 5 Capillary interactions between two patchy hexagram particles with PRs = 0.14 and 0.32 patches. (A) Experimental snapshots as the two particles approach one another. (B) Log-log plot for separation (r) as a function of $t_{max} - t$, where t_{max} is the time when the two particles make contact.

Interestingly, it has been reported that the value of $\beta = 12$ corresponds to pair interactions between dodecapolar interface deformations around interface-trapped spherical particles.⁵⁶

More importantly, the dodecapolar interactions between particles were indeed consistent with the formation of ordered suprastructures because of the directionality of the interactions. The nonlinear behavior in the small separation regime likely resulted from the rotation of hexagram particles to form additional tip-to-tip bonds at small separations.

Conclusions

In conclusion, we have successfully demonstrated the directed assembly of patchy hexagram particles at an air-water interface via directional interactions. Our results reveal that chemical heterogeneity, in addition to shape anisotropy, is a critical factor that must be pre-programmed to enable the directed self-assembly of interface-trapped particles into complex arrangements. We show that controlling the size of patches is critical for enabling the directed assembly of particles into ordered suprastructures because of the sharpness of the interface deformation around the patches. This sharp interface deformation around each patch coupled with the hexagram shapes leads to dodecapolar capillary attraction, enabling the directed self-assembly of patchy hexagram particles into hexagonal lattices.

Acknowledgements

This work was supported by the Basic Science Research Program through the National Research Foundation of Korea (NRF), which was funded by the Ministry of Science, ICT & Future Planning (MSIP) (No. NRF-2011-0017322). This work was also supported by the Space Core Technology Program through the National Research Foundation of Korea (NRF), which was funded by the Ministry of Science, ICT & Future Planning (NRF-2013M1A3A3A02042262).

Notes and references

a Department of Chemical Engineering, Chungnam National University, Yuseong-gu, Daejeon 305-764, Republic of Korea, E-mail: rhadum@cnu.ac.kr; Tel: +82-42-821-5896.
 b Department of Chemical Engineering, Kyung Hee University, Yongin-si, Gyeonggi-do, 446-701, Republic of Korea
 c Department of Chemical and Biomolecular Engineering, University of Pennsylvania, Philadelphia, 19104, United States

1. X. Mao, Q. Chen and S. Granick, *Nat. Mater.*, 2013, **12**, 217-222.
2. H. Onoe, K. Matsumoto and I. Shimoyama, *J. Microelectromech. Syst.*, 2004, **13**, 603-611.
3. G. M. Whitesides and B. Grzybowski, *Science*, 2002, **295**, 2418-2421.
4. Y. Min, M. Akbulut, K. Kristiansen, Y. Golan and J. Israelachvili, *Nat. Mater.*, 2008, **7**, 527-538.
5. S. C. Glotzer, *Science*, 2004, **306**, 419-420.
6. O. D. Velev and S. Gupta, *Adv. Mater.*, 2009, **21**, 1897-1905.
7. J. Kim, M. S. Oh, C.-H. Choi, S.-M. Kang, M. J. Kwak, J. B. You, S. G. Im and C.-S. Lee, *Soft Matter*, 2015, **11**, 4952-4961.
8. S. Park, J.-H. Lim, S.-W. Chung and C. A. Mirkin, *Science*, 2004, **303**, 348-351.

9. K. Miszta, J. Graaf, G. Bertoni, D. Dorfs, R. Brescia, S. Marras, L. Ceseracciu, R. Cingolani, R. Roij, M. Dijkstra and L. Manna, *Nat. Mater.*, 2011, **10**, 872-876.
10. Y. Nakagawa, H. Kageyama, Y. Oaki and H. Imai, *J. Am. Chem. Soc.*, 2014, **136**, 3716-3719.
11. O. D. Velev, *Science*, 2006, **312**, 376-377.
12. E. V. Shevchenko, D. V. Talapin, N. A. Kotov, S. O'Brien and C. B. Murray, *Nature*, 2006, **439**, 55-59.
13. A.-P. Hynninen, J. H. J. Thijssen, E. C. M. Vermolen, M. Dijkstra and A. van Blaaderen, *Nat. Mater.*, 2007, **6**, 202-205.
14. S.-H. Kim, W. C. Jeong, H. Hwang and S.-M. Yang, *Angew. Chem. Int. Ed.*, 2011, **50**, 11649-11653.
15. J.-G. Park, S.-H. Kim, S. Magkiriadou, T. M. Choi, Y.-S. Kim and V. N. Manoharan, *Angew. Chem.*, 2014, **126**, 2943-2947.
16. Q. Chen, S. C. Bae and S. Granick, *Nature*, 2011, **469**, 381-384.
17. S. Jain and F. S. Bates, *Science*, 2003, **300**, 460-464.
18. K. E. Jensen, D. Pennachio, D. Recht, D. A. Weitz and F. Spaepen, *Soft Matter*, 2013, **9**, 320-328.
19. P. Yin, H. M. T. Choi, C. R. Calvert and N. A. Pierce, *Nature*, 2008, **451**, 318-322.
20. F. Li, D. P. Josephson and A. Stein, *Angew. Chem. Int. Ed.*, 2011, **50**, 360-388.
21. R. Pasquino, F. Snijkers, N. Grizzuti and J. Vermant, *Langmuir*, 2010, **26**, 3016-3019.
22. L. Cademartiri and K. J. M. Bishop, *Nat. Mater.*, 2015, **14**, 2-9.
23. S. C. Glotzer and M. J. Solomon, *Nat. Mater.*, 2007, **6**, 557-562.
24. S. Sacanna and D. J. Pine, *Curr. Opin. Colloid Interface Sci.*, 2011, **16**, 96-105.
25. Y. Wang, Y. Wang, D. R. Breed, V. N. Manoharan, L. Feng, A. D. Hollingsworth, M. Weck and D. J. Pine, *Nature*, 2012, **491**, 51-55.
26. Z. Mao, H. Xu and D. Wang, *Adv. Funct. Mater.*, 2010, **20**, 1053-1074.
27. Y.-S. Cho, S.-H. Kim and J. H. Moon, *Korean J. Chem. Eng.*, 2012, **29**, 1102-1107.
28. C.-H. Choi, J. Lee, K. Yoon, A. Tripathi, H. A. Stone, D. A. Weitz and C.-S. Lee, *Angew. Chem.*, 2010, **122**, 7914-7918.
29. Z. Zhang, A. S. Keys, T. Chen and S. C. Glotzer, *Langmuir*, 2005, **21**, 11547-11551.
30. Z. Wang, X. Ke, Z. Zhu, F. Zhang, M. Ruan and J. Yang, *Phys. Rev. B*, 2000, **61**, R2472.
31. C. Richard, *Science*, 2003, **300**, 775-778.
32. K. P. Loh, Q. Bao, G. Eda and M. Chhowalla, *Nat. Chem.*, 2010, **2**, 1015-1024.
33. Y. Zhou, J. Park, J. Shi, M. Chhowalla, H. Park, D. A. Weitz and S. Ramanathan, *Nano Lett.*, 2015, **15**, 1627-1634.
34. T. Nguyen-Phan, V. H. Pham, H. Yun, E. J. Kim, S. H. Hur, J. S. Chung and E. W. Shin, *Korean J. Chem. Eng.*, 2011, **28**, 2236-2241.
35. J. H. Jeong, D.-W. Jung, B.-S. Kong, C. M. Shin and E.-S. Oh, *Korean J. Chem. Eng.*, 2011, **28**, 2202-2205.
36. M. Cavallaro, L. Botto, E. P. Lewandowski, M. Wang and K. J. Stebe, *Proc. Natl. Acad. Sci. USA*, 2011, **108**, 20923-20928.
37. E. M. Furst, *Proc. Natl. Acad. Sci. USA*, 2011, **108**, 20853-20854.
38. E. P. Lewandowski, M. Cavallaro Jr., L. Botto, J. C. Bernate, V. Garbin and K. J. Stebe, *Langmuir*, 2010, **26**, 15142-15154.
39. D. Ershov, J. Sprakel, J. Appel, M. A. Cohen Stuart and J. van der Gucht, *Proc. Natl. Acad. Sci. USA*, 2013, **110**, 9220-9224.
40. N. Bowden, A. Terfort, J. Carbeck and G. M. Whiteside, *Science*, 1997, **276**, 233-235.
41. R. Van Hooghten, L. Imperiali, V. Boeckx, R. Sharma and J. Vermant, *Soft Matter*, 2013, **9**, 10791-10798.
42. B. Madivala, J. Fransaer and J. Vermant, *Langmuir*, 2009, **25**, 2718-2728.
43. J. C. Loudet, A. M. Alsayed, J. Zhang and A. G. Yodh, *Phys. Rev. Lett.*, 2005, **94**, 018301.
44. J. C. Loudet, A. G. Yodh and B. Pouligny, *Phys. Rev. Lett.*, 2006, **97**, 018304.
45. Z. Zhang, P. Pfliegerer, A. B. Schofield, C. Clasen and J. Vermant, *J. Am. Chem. Soc.*, 2011, **133**, 392-395.
46. R. McGorty, J. Fung, D. Kaz and V. N. Manoharan, *Mater. Today*, 2010, **13**, 34-42.
47. B. J. Park, C.-H. Choi, S.-M. Kang, K. E. Tettey, C.-S. Lee and D. Lee, *Soft Matter*, 2013, **9**, 3383-3388.
48. B. J. Park, C.-H. Choi, S.-M. Kang, K. E. Tettey, C.-S. Lee and D. Lee, *Langmuir*, 2013, **29**, 1841-1849.
49. S.-M. Kang, A. Kumar, C.-H. Choi, K. E. Tettey, C.-S. Lee, D. Lee and B. J. Park, *Langmuir*, 2014, **30**, 13199-13204.
50. B. J. Park and E. M. Furst, *Soft Matter*, 2010, **6**, 485-488.
51. D. Stamou, C. Duschl and D. Johannsmann, *Phys. Rev. E*, 2000, **62**, 5263-5272.
52. S. Razavi, J. Koplik and I. Kretzschmar, *Soft Matter*, 2013, **9**, 4585-4589.
53. J.-Y. Wang, Y. Wang, S. S. Sheiko, D. E. Betts and J. M. DeSimone, *J. Am. Chem. Soc.*, 2012, **134**, 5801-5806.
54. D. C. Duffy, J. C. McDonald, O. J. A. Schueller and G. M. Whitesides, *Anal. Chem.*, 1998, **70**, 4974-4984.
55. J. C. Crocker and D. G. Grier, *J. Colloid Interface Sci.*, 1996, **179**, 298-310.
56. K. D. Danov, P. A. Kralchevsky, B. N. Naydenov and G. Brenn, *J. Colloid Interface Sci.*, 2005, **287**, 121-134.
57. C.-H. Choi, J. Kim, S.-M. Kang, J. Lee and C.-S. Lee, *Langmuir*, 2013, **29**, 8447-8451.
58. C.-H. Choi, J.-M. Jeong, S.-M. Kang, C.-S. Lee and J. Lee, *Adv. Mater.*, 2012, **24**, 5078-5082.
59. C.-H. Choi, S.-M. Kang, S. H. Jin, H. Yi and C.-S. Lee, *Langmuir*, 2015, **31**, 1328-1335.
60. M. Lee, D. Lee and B. J. Park, *Soft Matter*, 2015, **11**, 318-323.

61. A. H. Gröschel, A. Walther, T. I. Löbbling, J. Schmelz, A. Hanisch, H. Schmalz and A. H. E. Müller, *J. Am. Chem. Soc.*, 2012, **134**, 13850-13860.
62. V. N. Paunov and O. J. Cayre, *Adv. Mater.*, 2004, **16**, 788-791.
63. B. P. Binks, *Curr. Opin. Colloid Interface Sci.*, 2002, **7**, 21-41.
64. P. A. Kralchevsky and N. D. Denkov, *Curr. Opin. Colloid Interface Sci.*, 2001, **6**, 383-401.
65. C. A. Schneider, W. S. Rasband and K. W. Eliceiri, *Nat. Methods*, 2012, **9**, 671-675.